© MAR 2020 | IRE Journals | Volume 3 Issue 9 | ISSN: 2456-8880

A Novel Three-Phase Transfer Field Reluctance Motor – An Evaluation of Its Performance Characteristics

OBUTE K. C.[1], OLUFOLAHAN ODUYEMI[2], ELEANYA M.N[3], ANIONOVO U.E[4]

[1, 3, 4] *Department of Electrical Engineering, Nnamdi Azikiwe University, Awka*

[2] *Department of Engineering and Technology, South East Missouri State University, Cape Giradeau, Missouri, USA*

***Abstract-* The ultimate parameter, upon which every rotating electric machine is scaled is its performance characteristics, which includes; the output torque, output power, angular speed, power factor and efficiency. Obviously, the output characteristics of all conventional transfer field effect machines are much inferior to that of conventional induction machines of comparable sizes and ratings. This is a consequence of their low direct axis reactance to quadrature axis reactance ratio, coupled with the excessive leakage reactance from the quadrature axis reactance. This is because they possess projected rotor pole structures. An analysis of the afore-mentioned, using dynamic/steady state models is the subject matter of this work. This is achieved by transformation of the machine's parametric equations in a-b-c reference frame to arbitrary q-d-o reference frame, from which its equivalent circuit/matlab simulation/plots were obtained.**

***Indexed Terms-* Transfer field motor, reference frame, dynamic/steady-state model, equivalent circuit.**

I. INTRODUCTION

In its broad definition, a reluctance motor is electric machine in which torque is produced by the tendency of a movable part to move into a position where the inductance of an energized phase winding is a maximum. In its familiar form, it is a three-phase machine with salient (projected) pole rotor structure having a squirrel cage which is included only for the purpose of enabling it to start as an asynchronous machine and then pull into synchronous at fuel speed (Ijeomah, C. N. et al, 1996). Structurally, the transfer field motor is basically a reluctance machine. It differs from the simple reluctance machine in two important aspects viz;

i) it has two set of windings instead of one, as obtainable in simple reluctance machine
ii) each winding has a synchronous reactance which is independent of rotor position, unlike the winding reactance of simple reluctance machine that varies cyclically (L.A. Agu, 1984). The transfer field reluctance machines occupy a very lowly position in the family of rotating electric machinery because of its low output characteristics in comparison with an induction machine of the same dimension. Despite these setbacks, transfer field effect motors are almost the inevitable choice in electric clocks, textile drives, grinding machines for perishables etc.

II. MACHINE DESCRIPTION/PHYSICAL CONFIGURATION

The transfer field reluctance machine (TFM) as shown in Plate 1 with connection diagram as in figure 1, comprises a two stack machine in which the rotor is made up of two identical equal halves whose pole axes are $\pi/2$ radians out of phase in space. They are housed in their respective induction motor type stators. There are no windings in the rotor. The stator has two physically isolated but magnetically coupled identical windings known as the main and auxiliary windings. The axes of the main windings are the same in both halves of the machine, whereas the axes of the auxiliary windings are transposed in passing from one half of the machine to the other. Both sets of windings are distributed in the stator slots and occupy the same slots for perfect coupling and have the same number of poles. The two sets of windings of the transfer field machine are essentially similar and may be connected in parallel which of course double its output.

The stator and rotor of the machine are wound for the same pole number and both are star connected as in fig 1.

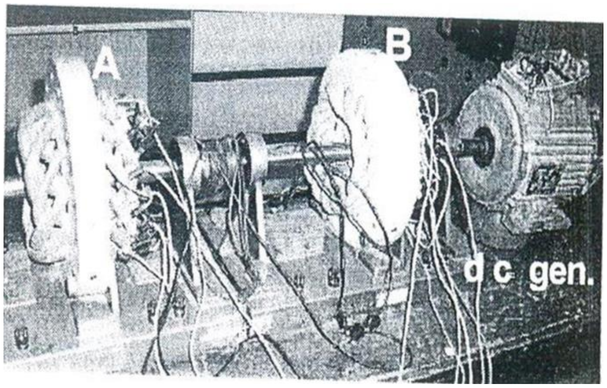

Plate 1 – Pictorial view of a transfer field reluctance machine. Courtesy of machine laboratory, University of Nigeria Nsukka

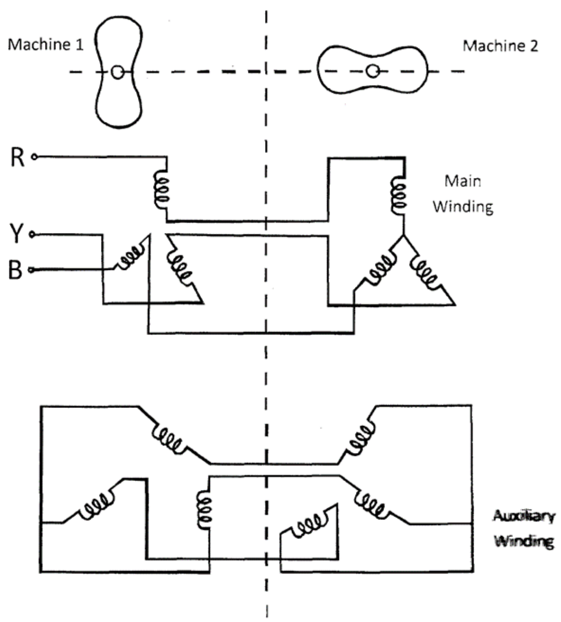

Fig 1 Connection diagram for a transfer field motor (Eleanya M.N 2015)

III. THE MACHINE MODEL

The per-phase coupled coil representation of the Transfer Field Machine is shown in fig 2 below

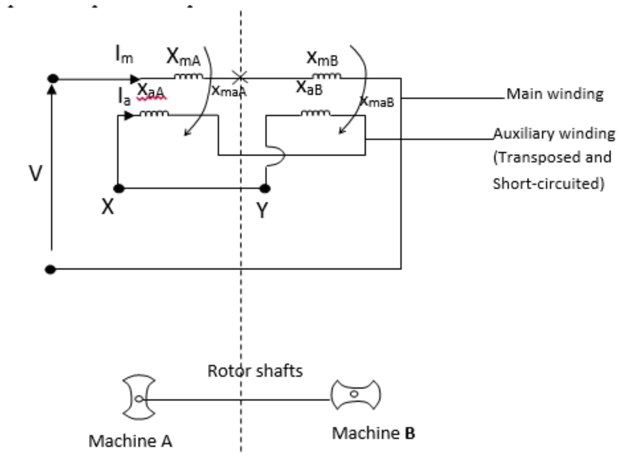

Fig 2: Per phase coupled coil representation of a T.F. Motor

Each machine half is similar in features to the conventional synchronous machine. The major unorthodox characteristics of the machine are;

i) the stator and rotor are arranged in two identical halves; and hence the machine may be treated as two separate reluctance machines whose stator windings are connected in series.
ii) there are no windings in the rotor
iii) the pole axes of the two pole half are mutually in space quadrature there is second set of poly-phase stator windings (auxiliary windings) whose conductor side are shifted electrical by 180^0 (anti-series), by passing through one section of the machine to another. The main and the auxiliary windings are identical in all respects and occupy the same electrical position in the stator slot, thus ensuring a perfect coupling between the windings.

IV. PRINCIPLE OF OPERATION AND ANALYSIS

The analysis of the three-phase transfer-field machine derived from the studies on coupled machines (Anih L.U. et al 2001).

In its operation, when the main windings of machine **A** is connected to an **a.c** supply voltage, V, with the auxiliary windings open circuited, it draw a magnetizing current $\mathbf{I_o}$ at the supply frequency $\boldsymbol{\omega_o}$.

This magnetizing current produces an magnetomotive force (mmf) distribution on both units of the machine

(A and B) which may be expressed as (Anih L.U. et al 2008);

Magnetizing (mmf) $m_o = M_o \cos (x - \omega_o t)$ (1)

Where; m_0 = Instantaneous value of the magnetizing mmf

M_o = Peak amplitude of the instantaneous magnetizing mmf

x = Angular distance measured from the reference axis, which is taken as the center line of the stator poles

t = Time in seconds

ω_0 = Supply angular frequency.

The air-gap permeance of the rotor in one unit machine, say unit A, may be expressed as;

$P_A = P_o + P_V \cos 2 (x-\omega t)$ (2)

Where;

P_A = Rotor permeance distribution for unit area of air-gap of machine **A** half.

P_v = the amplitude of the variable part of the permeance distribution.

ω = the speed of rotor of unit machine

Similarly, the air-gap rotor permeance distribution in unit B machine, whose pole axis is in space quadrature with unit A machine may be expressed as;

$P_B = P_o + P_v \cos 2 (x - \omega t - 90^0)$

$= P_o - P_v \cos 2 (x - \omega t)$ (3)

The flux density produced by this mmf at the instant when its axis coincides with the pole axis of the rotor of machine A is given by;

$B_{AO} = m_o P_A$

$= M_0 \cos (x-\omega_o t) [P_o + P_V \cos 2 (x-\omega t)]$

$= M_o P_o \cos (x-\omega_o t) + M_o P_V \cos (x-\omega_o t) \cos 2 (x-\omega t)$

$= M_o P_o \cos (x-\omega_o t) + 0.5 M_o P_V \cos [x - (2\omega - \omega_o)t]$

$+ 0.5 M_o P_V \cos (3x - \omega t - \omega t)$ + third harmonics

(4)

Similarly, the corresponding flux density distribution produced in machine B is expressed as;

$B_{BO} = M_o P_o \cos (x-\omega_o t) - 0.5 M_o P_o \cos [x + (\omega_o - 2\omega)t]$ + third space harmonics

(5)

It should be noted at this juncture that the first components of equations (4 and 5) will induce emfs E_1 in the main windings which is additive and tend to oppose the voltage supply. The e.mf's they induce in the auxiliary windings cancel out. These e.m.fs are equal in magnitude and in time phase.

The second components of equations (4 and 5), will induce voltages E_2, in the main windings which are equal and opposite and in consequence, cancel each other (anti-phase). However, in he auxiliary winding, these induced voltages, E_2 will add up because of the transposition of the auxiliary windings. See fig 3 for illustration.

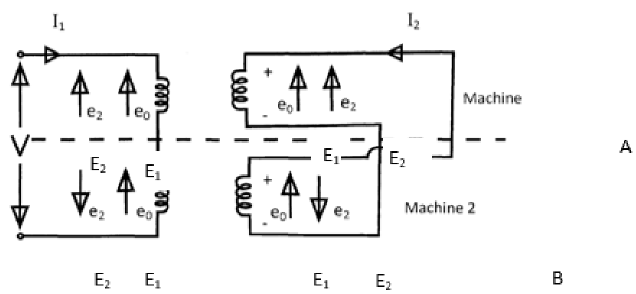

Fig 3: Induced voltage, E_1, E_2 in the main and auxiliary winding

The direction of emf E_1 induced in the main winding conductor in both halves of the machine A, B such as a_1 and $\acute{a}_1$ by this flux is as shown in fig 3 in full lines. These emfs E_1 are both equal in magnitude and in time phase in both sections of the machine and will oppose the supply voltage V in both sections

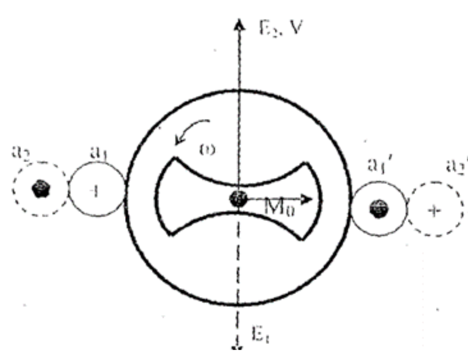

Fig 4a: Section A part of the machine showing the induced e.m.f s in the stator windings

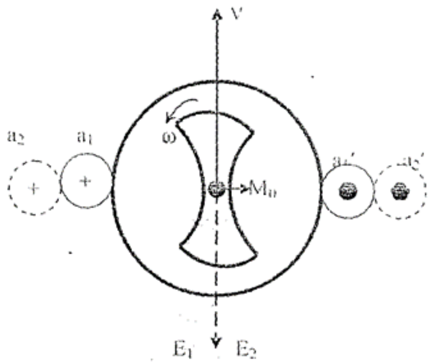

Fig 4b: Section B part of the machine showing the induced e.m.f s in the stator windings (Source- Anih/Agu 2008)

The emfs induced by the third space harmonics cancel out if the windings are star connected. If however, the windings are desired to be connected in delta, the winding pitch must be chosen such that the emf induced by harmonics of flux is eliminated.

The average value of the second components of the flux in equation (4 and 5);

ie $\pm 0.5\, M_o\, P_o \cos[x + (\omega_o - 2\omega)t] = 0$

More-still, the average of this flux as seen by the auxiliary windings, whose conductors are transposed between the two machine halves is expressed as;
$B_{AO} - B_{BO} = 0.5\, M_o\, P_V \cos[x + (\omega_o - 2\omega)t]$ (6)

This flux density distribution rotates in the negative clockwise direction for $\omega < \frac{\omega_o}{2}$

The direction of emf E_2 induced in the auxiliary windings by this flux will be in anti-phase in both halves of the machine (see fig 3), because of the transposition of the auxiliary windings as shown in the dotted circles in fig 4b It therefore follows that in section A half, E_2 will be diametrically opposed to E_1 and in section B half E_2 will be in phase with E_1 (see fig.3)

V. THE DYNAMIC MODEL OF 3-PHASE TRANSFER FIELD MOTOR

For the stator windings of the three-phase TF machine, the mathematical model of the voltage equation is given by;

$V_A = r_A i_A + P\lambda_A$ (7)

$V_B = r_B i_B + P\lambda_B$ (8)

$V_C = r_C i_C + P\lambda_C$ (9)

Where $V_A = V_R$ (Red)
$V_B = V_Y$ (yellow)

$V_C = V_B$ (Blue) are the three phase balance voltage which rotate at the supply frequency (ω) at the main winding.

For the rotor, the flux linkages rotate at the speed of the rotor (ω_r).

Therefore for the auxiliary winding of the machine, we have;

$V_a = r_a i_a + \rho\lambda_a$ (10)

$V_b = r_b i_b + \rho\lambda_b$ (11)

$V_c = r_c i_c + \rho\lambda_c$ (12)

Equations (7-12) can be written in a compact form as;

$V_{ABC} = r_{ABC}\, i_{ABC} + \rho\lambda_{ABC}$ (13)

$V_{abc} = r_{abc}\, i_{abc} + \rho\lambda_{abc}$ (14)

where;
$\rho = d/dt$ (derivative term, as usual)

$(V_{ABC})^T = [V_A, V_B, V_C]$ (15)

$(V_{abc})^T = [V_a, V_b, V_c]$ (16)

$r_{ABC} = \mathrm{diag}([r_A\, r_B\, r_C])$ (17)

$r_{abc} = \mathrm{diag}([r_a\, r_b\, r_c])$ (18)

In the above two equations (15) and (16), "ABC" subscript denotes variables and parameters associated with the main winding and the subscript "abc" denotes variables and parameters associated with the auxiliary winding. Both r_{ABC} and r_{abc} are diagonal matrices each with equal non zero element. For a magnetically linear system, the flux linkages may be expressed as (Anih L.U, Obe E.S. 2009);

$$\begin{bmatrix} \lambda_{ABC} \\ \lambda_{abc} \end{bmatrix} = \begin{bmatrix} L_{GG} & L_{GH} \\ L_{HG} & L_{HH} \end{bmatrix} \begin{bmatrix} i_{ABC} \\ i_{abc} \end{bmatrix} \text{ wb turn} \quad (19)$$

Where,

$$\left.\begin{aligned} \lambda_{ABC} &= (\lambda_A, \lambda_B, \lambda_C)^t \\ \lambda_{abc} &= (\lambda_a, \lambda_b, \lambda_c)^t \\ i_{ABC} &= (i_A, i_B, i_C)^t \\ i_{abc} &= (i_a, i_b, i_c)^t \end{aligned}\right\} \quad (20)$$

The super-script t of equation (20) denotes the transpose of the array.

The inductance matrices term L_{GG} , L_{GH}, and L_{HH} are obtained from inductance sub-matrices L_{11}, L_{12}, L_{21} and L_{22} for machines A and B, defined as;

$$\left.\begin{aligned} L &= \begin{bmatrix} L_{11} & L_{12} \\ L_{21} & L_{22} \end{bmatrix} \\ L_{11} &= \begin{bmatrix} L_{AA} & L_{AB} & L_{AC} \\ L_{BA} & L_{BB} & L_{BC} \\ L_{CA} & L_{CB} & L_{CC} \end{bmatrix} \\ L_{12} &= \pm \begin{bmatrix} L_{Aa} & L_{Ab} & L_{Ac} \\ L_{Ba} & L_{Bb} & L_{Bc} \\ L_{Ca} & L_{Cb} & L_{Cc} \end{bmatrix} \\ L_{21} &= \pm \begin{bmatrix} L_{aA} & L_{aB} & L_{aC} \\ L_{bA} & L_{bB} & L_{bC} \\ L_{cA} & L_{cB} & L_{cC} \end{bmatrix} \\ L_{22} &= \begin{bmatrix} L_{aa} & L_{ab} & L_{ac} \\ L_{ba} & L_{bb} & L_{bc} \\ L_{ca} & L_{cb} & L_{cc} \end{bmatrix} \end{aligned}\right\} \quad (21)$$

Where;

L = the augmented matrix, for the inductance matrix for machine A and B

L_{11} and L_{22} are "self" inductances of main and auxiliary windings respectively.

L_{12} and L_{21} are the "mutual" inductances between the main and auxiliary windings.

L_{GG} is obtained by adding L_{11} for machine A and L_{11} for machine B.

This will yield;

$$L_{GG} \begin{bmatrix} (2L_{Ls}+L_{md}+L_{mq}) & -\frac{1}{2}(L_{md}+L_{mq}) & -\frac{1}{2}(L_{md}+L_{mq}) \\ -\frac{1}{2}(L_{md}+L_{mq}) & (2L_{Ls}+L_{md}+L_{mq})a & -\frac{1}{2}(L_{md}+L_{mq}) \\ -\frac{1}{2}(L_{md}+L_{mq}) & -\frac{1}{2}(L_{md}+L_{mq}) & (2L_{Ls}+L_{md}+L_{mq}) \end{bmatrix} \quad (22)$$

L_{GH} is obtained by adding L_{12} for machine A to L_{12} for machine B to give

$$L_{GH} = (L_{mq} - L_{md}) \begin{bmatrix} \cos 2\theta r & \cos(2\theta r-\alpha) & \cos(2\theta r+\alpha) \\ \cos(2\theta r-\alpha) & \cos(2\theta r+\alpha) & \cos 2\theta r \\ \cos(2\theta r+\alpha) & \cos 2\theta r & \cos(2\theta r-\alpha) \end{bmatrix} \quad (23)$$

Where $\alpha = \frac{2\pi}{3}$

By applying the same method, L_{HG} and L_{HH} are obtained. So far the main and auxiliary windings in both machine halves are identical, L_{GG} is observed to be equal to L_{HH}. So also L_{GH} and L_{HG}. Owing to this observation of equality, auxiliary winding parameters do not change values when they are referred to the main winding. Equations (22) and (23) resemble the inductance expressions for a wound rotor induction machine, even though the individual machine making up the composite machine possesses salient pole rotors with no conductors.

VI. MACHINE MODEL IN ARBITRARY Q-D-O REFERENCE FRAME

In order to remove the rotor position dependence on the inductance seen in equation (23), the voltage equations (13) and (14) need to be transferred to q-d-o reference frame. The technique is to transform all the state variables to an arbitrary reference frame. Equation (19) is then rewritten in q-d-o frame as;

$$\begin{bmatrix} (\lambda_Q & \lambda_D & \lambda_O) \\ (\lambda_q & \lambda_d & \lambda_o) \end{bmatrix}^T = \begin{bmatrix} K_G L_{GG}\,(k_G)^{-1} & K_G L_{GH}\,(k_H)^{-1} \\ K_G L_{GH}\,(k_G)^{-1} & K_G L_{HH}\,(k_H)^{-1} \end{bmatrix} \begin{bmatrix} (I_Q & I_D & I_O) \\ (I_q & I_d & I_o) \end{bmatrix} \quad (24)$$

$$\left.\begin{aligned} &\text{Here, } K_G = \frac{2}{3}\begin{bmatrix} \mathrm{Cos}\,\phi & Cos\,(\phi-\alpha) & Cos\,(\phi+\alpha) \\ \mathrm{Sin}\,\phi & Sin\,(\phi-\alpha) & Sin\,(\phi+\alpha) \\ \frac{1}{2} & \frac{1}{2} & \frac{1}{2} \end{bmatrix} \\ &K_H = \frac{2}{3}\begin{bmatrix} \mathrm{Cos}\,\beta & Cos\,(\beta-\alpha) & Cos\,(\beta+\alpha) \\ \mathrm{Sin}\,\beta & Sin\,(\beta-\alpha) & Sin\,(\beta+\alpha) \\ \frac{1}{2} & \frac{1}{2} & \frac{1}{2} \end{bmatrix} \\ &\text{Where, } \theta_r = \text{rotor position} \end{aligned}\right\} \quad (25)$$

β = speed of rotation of the arbitrary reference frame.

As $\beta = 2\theta_r = \theta$, as in equation (23) the time varying inductance frame, the voltage equation will be totally eliminated.

Hence, the voltage equations (13) and (14) will after the transformation yield;

$V_Q = \omega\lambda_D + \rho\lambda_Q + rI_Q$ (26)

$V_D = \omega\lambda_Q + \rho\lambda_D + rI_D$ (27)

$V_O = \rho\lambda_O + rI_O$ (28)

Doing like-wise for the rotor quantities (auxiliary windings) yield;

$V_q = (\omega\text{-}2\omega_r)\,\lambda_d + \rho\lambda_q + rI_q$ (29)

$V_d = (\omega\text{-}2\omega_r)\,\lambda_q + \rho\lambda_d + rI_d$ (30)

$V_o = (\omega\text{-}2\omega_r)\,\rho\lambda_o + rI_o$ (31)

Also, the flux linkages of equation (23) are expressed as;

$\lambda_Q = (2L_1 + L_{mq} + L_{md})I_Q - (L_{md} - L_{mq})I_q$

$= 2\,L_1\,I_Q + L_{mq}\,I_Q + L_{md}\,I_Q - L_{md}\,I_q + L_{mq}\,I_q$

$= 2\,L_1\,I_Q + L_{mq}\,I_Q + L_{md}\,I_Q + L_{md}\,I_Q - L_{md}\,I_Q - L_{md}\,I_q + L_{mq}\,I_q$

$= 2\,L_1\,I_Q + 2L_{md}\,I_Q + L_{mq}\,I_Q - L_{md}\,I_Q - L_{md}\,I_q + L_{mq}\,I_q$

$= 2(L_1 + L_{md})\,I_Q + [I_Q\,(L_{mq}+L_{md}) + I_q\,(L_{mq} - L_{md})]$

$= 2\,(L_1 + L_{md})\,I_Q + (I_Q+L_q)\,(L_{mq} - L_{md})$

$\Rightarrow \lambda_Q = 2(L_1 + L_{md})\,I_Q + (I_Q+I_q)\,(L_{mq} - L_{md})$ (32)

Similarly

$\lambda_D = (2L_1 + L_{mq} + L_{md})\,I_D + (L_{md} - L_{mq})\,I_d$

$\Rightarrow \lambda_D = 2(L_1 + L_{mq})\,I_D + (I_D - I_d)\,(L_{md} - L_{mq})$ (33)

$\lambda_O = 2L_1\,I_O$ (34)

Also

$\lambda_q = (2L_1 + L_{mq} + L_{md})\,I_q - (L_{md} - L_{mq})\,I_Q$

$= 2(L_1 + L_{md})\,I_q + (L_{mq} - L_{md})\,(I_Q+I_q)$ (35)

$\lambda_d = (2L_1 + L_{mq} + L_{md})\,I_d + (L_{md} - L_{mq})\,I_D$

$= 2(L_1 + L_{mq})\,I_d + (L_{md} - L_{mq})\,(I_D+I_d)$ (36)

$\lambda_O = 2L_1 I_O$ (37)

As before, equations (32– 34) represent the flux linkages of the main winding circuit while equations

(35 – 37) represent the flux linkages of the auxiliary winding, and **r** in equations (26 – 31) is the sum of the resistances of the main or auxiliary windings in both machine halves.

Hence, equation (32) can be put into equation (26), and equations (36) into equation (29) to yield;

$V_Q = \omega\lambda_D + \rho\ [2(L_1 + L_{md})\ I_Q + (L_{mq} - L_{md})\ (I_Q + I_q)] + rI_Q$

$= \omega\lambda_D + j\omega\ [2(L_1 + L_{md})]\ I_Q + j\omega\ (L_{mq} - L_{md})\ (I_Q + I_q) + rI_Q$ (38)

$\Rightarrow V_q = (\omega - 2\omega_r)\ \lambda_d + \rho\ [2(L_1 + L_{md})\ I_q] + (L_{mq} - L_{md})\ (I_Q + I_q)] + rI_q$

$\therefore V_q = (\omega - 2\omega_r)\ \lambda_d + j\omega\ [2(L_1 + L_{mq})]\ I_q + j\omega\ (L_{mq} - L_{md})\ (I_Q + I_q) + rI_q$ (39)

Equation (38) and (39) result the T equivalent circuit shown below in figure 5.

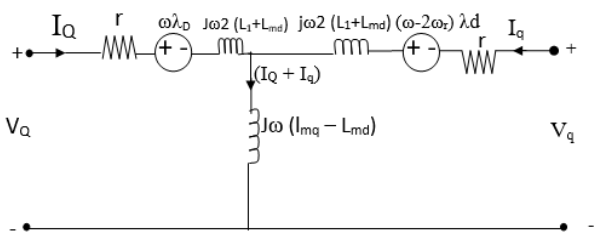

Fig 5: Arbitrary reference frame equivalent circuit for a 3-phase symmetrical transfer field machine in the q-variable.

Applying the same method to equation (33) and (27) and then equations (35) and (30) we have;

$V_D = -\ \omega\lambda_Q + \rho\ [2(L_1 + L_{mq}) + (L_{md} - L_{mq})\ (I_D + I_d)] + rI_D$

$= -\ \omega\lambda_Q + j\omega 2\ (L_1 + L_{mq})\ I_D + j\omega\ (L_{md} - L_{mq})\ (I_D + I_d) + rI_D$ (40)

$V_d = -\ (\omega - 2\omega_r)\ \lambda_q + \rho\ [2(L_1 + L_{mq})\ I_q + (L_{md} - L_{mq})\ (I_D + I_d)] + rI_d$

$= -\ (\omega - 2\omega_r)\ \lambda_q + j\omega 2\ (L_1 + L_{mq})\ I_q + j\omega\ (L_{md} - L_{mq})\ (I_D + I_d)] + rI_d$ (41)

Equations (40) and (41) result the Tequivalent circuit shown below in figure 6

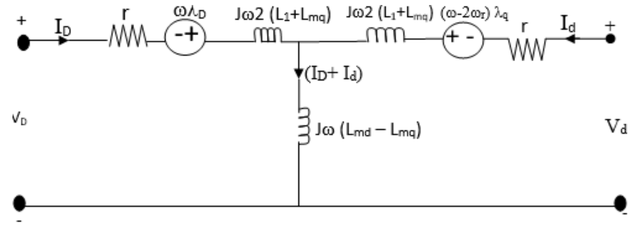

Fig 6: Arbitrary reference frame equivalent circuit for a 3-phase symmetrical transfer field machine in the d-variables

More still, from equation (28) and (34), (31) and (37) we have;

$V_o = \rho\lambda_o + rI_o$

$= \rho(2L_1\ I_o) + rI_o$ (42)

$V_{or} = \rho\lambda_o + rI_o$

$= \rho(2L_1\ I_o) + rI_o$ (43)

Equations (42) and (43) result the T equivalent circuit shown in fig 7

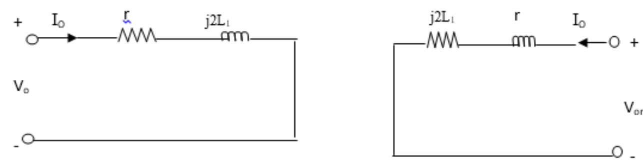

Fig.7: Arbitrary reference frame equivalent circuit for a 3 – phase symmetrical transfer field machine in the O-variable

VII. q-d-o Torque Equation

The expression for electromagnetic torque is obtained from energy considerations and derived to be (Anih L.U, Obe E.S 2009);

$$T_e = \frac{P_n}{2}\left[K_G\begin{pmatrix} I_A \\ I_B \\ I_C \end{pmatrix}\right]^T \left[\frac{\partial}{\partial\theta}\ [L_{GH}]\right]\left[K_G\begin{pmatrix} I_a \\ I_b \\ I_c \end{pmatrix}\right] \quad (44)$$

Equation (44) can be shown to yield;

$$T_e = \frac{3}{4}\ P_n\ (L_{md} - L_{mq})\ (I_Q\ I_d - I_q\ I_D) \quad (45)$$

Equation (45) shows that currents in both the main and auxiliary windings contribute positively to torque production, therefore, there is no copper penalty limitation of space for auxiliary winding conductor is utilized.

The electromechanical (rotor) dynamic equation for the machine is expressed as;

$J\frac{d\omega_m}{dt} = T_e - T_L$ (46)

Where;

P_n = Number of poles

T_L = motor shaft load torque in N-m

T_e = Electromagnetic torque in N-m

J = Moment of inertia of motor in kg – m^2

ω_m = Mechanical rotor speed in $rads^{-1}$

VIII. Steady-state analysis of 3-phase transfer field machine model in arbitrary q-d-o reference frame

The steady state equivalent circuit of a three-phase transfer field machine may be derived from the d-q-o equivalent circuit. This can be achieved with the understanding that all the derivative terms of equation (26) through equation (32) are set to zero, and the following relations exist between the q-axis and d-axis variables.

$F_D = jF_Q$ (Main winding circuit)

$F_d = - jF_Q$ (Auxiliary winding circuit)

$V_Q = V_A$, $I_Q = I_A$, $V_q = V_a$, $I_q = I_a$

As the machine is half speed type with synchronous speed $\omega^1 = \frac{\omega}{2}$; the per slip $\acute{s}$ is given by;

$\acute{s} = \frac{\acute{\omega}-\omega_r}{\acute{\omega}}$ (47)

$= \frac{0.5\omega-\omega_r}{0.5\omega}$

$= \frac{\omega-2\omega_r}{\omega}$

$\Rightarrow \acute{s}\omega = \omega-2\omega_r$ (48)

But for the normal induction machine counterpart;

$s = \frac{\omega-\omega_r}{\omega}$

$\Rightarrow \omega_r = \omega-s\omega$ (49)

Putting equation (49) into equation (48), yields;

$\acute{s} = 2s – 1$ (50)

It can be recalled from equations (26-32) that;

$V_Q = \omega\lambda_D + \rho\lambda_Q + rI_Q$

$= \omega\lambda_D + (0)\lambda_Q + rI_Q$

$= \omega\lambda_D + rI_Q$

$\Rightarrow V_Q = \omega\lambda_D + rI_Q$

$= j\omega [2 (L_1+ L_{mq}) I_D + (L_{md} - L_{mq}) (I_D+I_d)] + rI_Q$

$= j[2 (x_1+ x_{mq}) I_D + (x_{mq} - x_{md}) (I_D+I_d)] + rI_Q$

$\Rightarrow V_A = [j2(x_1+ x_{mq})+r] I_A + j (x_{md} - x_{mq}) (I_A+I_a)$

(51)

Similarly

$V_q = (\omega-2\omega_r) \lambda_d + \rho \lambda_d + rI_q$

$= (\omega-2\omega_r) \lambda_d + (0)\lambda_q + rI_q$

$= (\omega-2\omega_r) \lambda_d + rI_q$

$= \acute{s}\omega \lambda d+ rI_q$

$= j\acute{s}\omega [2(L_1+ L_{mq})) I_d + (L_{md} - L_{mq}) (I_D+I_d)] + rI_q$

$= j\acute{s} [2(x_1+ x_{mq})) I_d + (x_{md} - x_{mq}) (I_D+I_d) + rI_q$

Dividing both sides by $\acute{s}$, we have;

$\Rightarrow \frac{V_q}{\acute{s}} = j [2(x_1+ x_{mq})) I_d + (x_{md} - x_{mq}) (I_D+I_d) + \frac{rI_q}{\acute{s}}$

$\Rightarrow \frac{V_a}{\acute{s}} = [j2(x_1+ x_{mq})I_a] + j(x_{md} - x_{mq}) (I_A+I_a) +\frac{rI_a}{\acute{s}}$

$= [2j(x_1+ x_{mq}) + \frac{r}{\acute{s}}]I_a + j(x_{md} - x_{mq}) (I_A+I_a)]$

Referring to equation (50);

$\frac{V_a}{2S-1} = [j2(x_1+ x_{mq}) + \frac{r}{2S-1}] I_a + j [(x_{md} - x_{mq}) (I_A+I_a)]$

(52)

Equations (51) and (52) result a per phase T – equivalent circuit as shown in figure 8.

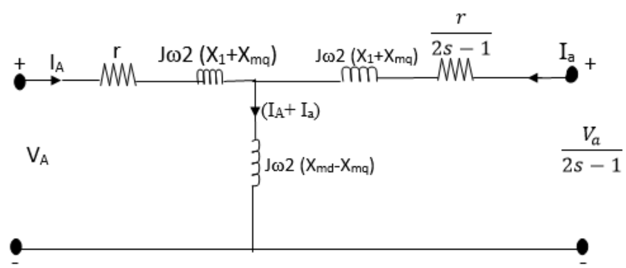

Fig 8: Per phase steady state T – equivalent circuit of a 3-phase transfer field machine, using the q-variable.

The rotor (auxiliary) is usually short circuited and hence from figure 8, $\frac{V_a}{2S-1} = 0$

Also, $\frac{r}{2S-1} = r + \frac{2r(1-s)}{2S-1}$ (53)

Hence, figure 8 can be redrawn for better as in figure 9 to suit equation (53) as below.

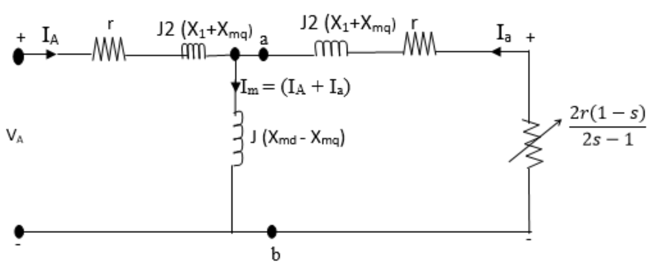

Fig 9. Per phase steady state T - equivalent circuit of a 3-phase transfer field motor.

N-B - Figure 9 can also be obtained using the d-variable of equation (27) and (30).

IX. Power across air – gap, Torque and power output in 3-phase Transfer field Machine

With reference to the equivalent circuit of figure (9), the power crossing the terminals (ab) in the circuit is the electrical power input per phase minus the stator losses (stator copper and iron losses) and hence, is the power that is transferred from the stator (main windings) to the rotor (auxiliary windings) through the air-gap magnetic field. This is known as the power across the air gap. Its 3-phase value is symbolized as P_G.

From figure 9,

$P_G = 3(I_a)^2 \frac{r}{2S-1}$ (54)

The Auxiliary winding copper loss $P_{c(aux)} = 3(I_a)^2\, r$ (55)

$\therefore$ From equations (54) and (55);

$P_G = \frac{P_c\,(aux)}{2S-1}$

$\Rightarrow P_c\,(aux) = (2S-1)P_G$ (56)

If equation (55) is subtracted from equation (54), we have;

$P_G - P_c\,(aux) = P_m$ (Mechanical output (gross) power)

$\Rightarrow P_m = [\,3(I_a)^2 \frac{r}{2S-1}] - [\,3(I_a)^2 r]$

$= 6(I_a)^2 \frac{r(1-s)}{2S-1}$

$\Rightarrow P_m = 2P_G\,(1-s)$ (57)

From the equations established so far, it is evident that high slip (s) operation of the transfer field machine would be highly inefficient, hence, transfer field motor just as the induction motor counterpart are therefore designed to operate at low slip at full load.

X. The steady-state output characteristic of a 3-phase transfer field reluctance motor

The steady-state output characteristic of a 3-phase transfer field reluctance machine can be studied for clarity if the per phase steady-state equivalent circuit of figure (9) is modified as shown fig 10 below; taking $x_1 + x_{mq} = x_q$

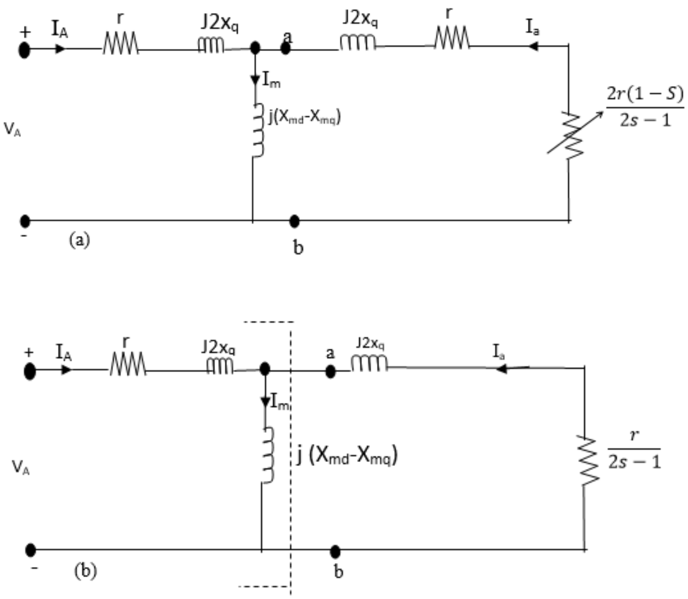

Fig 10a/b: Modified per phase steady-state T-equivalent circuit of a 3-phase transfer field motor.

From figure 10, the V_{TH} (voltage across a-b) is given by;

$V_{TH} = \left[\frac{j\,(X_{md}-X_{mq})}{j\,(X_{md}-X_{mq}) + (r+j2X_q)}\right] V_A$ volts

$= \left[\frac{j\,(X_{md}-X_{mq})}{r+j\,(X_{md}-X_{mq}+2X_q)}\right] V_A$ volts (58)

If $r \ll j\,(x_{md}-x_{mq}+2x_q)$, then equation (58) becomes;

$V_{TH} = \left[\frac{j\,(X_{md}-X_{mq})}{j\,(X_{md}-X_{mq}+2X_q)}\right] V_A$ volts (59)

$\Rightarrow V_{TH} = \left[\frac{(X_{md}-X_{mq})}{(X_{md}-X_{mq}+2X_q)}\right] VA$ volts

Also $Z_{TH} = \frac{j\,(X_{md}-X_{mq})(r+j\,2X_q)}{j\,(X_{md}-X_{mq}) + (r+j2X_q)}$

$= \frac{j\,(X_{md}-X_{mq})(r+j2X_q)}{r+j(X_{md}-X_{mq}+2X_q)}$ (60)

If $r \ll j\,(r_{md}-x_{mq}) + 2x_q$), then equation (58) become;

$Z_{TH} = \frac{j\,(X_{md}-X_{mq})(r+j2X_q)}{j\,(X_{md}-X_{mq}+2X_q)}$

$= \frac{(X_{md}-X_{mq})(r+j2X_q)}{(X_{md}-X_{mq}+2X_q)}$

$= \frac{r\,(X_{md}-X_{mq}) + j2X_q\,(X_{md}-X_{mq})}{(X_{md}-X_{mq}+2X_q)}$

$= \frac{r\,(X_{md}-X_{mq})}{(X_{md}-X_{mq}+2X_q)} + \frac{j(2X_q(X_{md}-X_{mq})}{(X_{md}-X_{mq}+2X_q)}$ (61)

But $Z_{TH} = R_{TH}$ (Real Component) + X_{TH} (Imaginary component)

Hence, $R_{TH} = \frac{r\,(X_{md}-X_{mq})}{X_{md}-X_{mq}+2X_q}$ (62)

$X_{TH} = \frac{j[(2X_q(X_{md}-X_{mq})]}{X_{md}-X_{mq}+2X_q}$ (63)

The circuit of figure (10b), then reduces to that of figure 11, in which it is convenient to take V_{TH} as the reference voltage

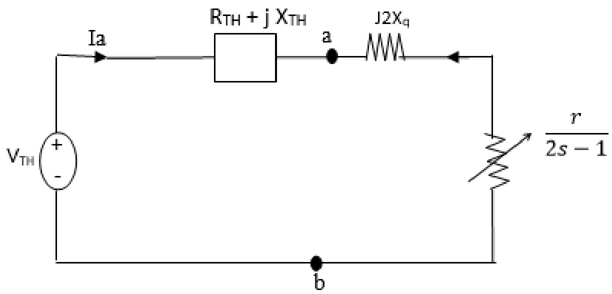

Fig 11: Thevenin equivalent of 3 – phase transfer field motor circuit model

From figure 11,

$$I_a = \frac{V_{TH}}{\left(R_{TH}+\frac{r}{2s-1}\right)+j(X_{TH}+2x_q)} \text{ Amperes} \quad (64)$$

$$\Rightarrow (I_a)^2 = \frac{(V_{TH})^2}{\left(R_{TH}+\frac{r}{2s-1}\right)^2+(X_{TH}+2x_q)^2} \text{ Amperes} \quad (65)$$

The expression for the steady state electromagnetic torque is given by;

$$T_e = \frac{P_m}{\omega_r} = \left(\frac{6(I_a)^2 r}{\omega_r}\right)\left(\frac{1-s}{2s-1}\right)$$

$$= \left(\frac{6(I_a)^2 r}{\omega\,(1-s)}\right)\left(\frac{1-s}{2s-1}\right) = \frac{6(I_a)^2 r}{\omega(2s-1)} \quad \text{N-m} \quad (66)$$

Hence, putting equation (65) into equation (66) yields;

$$T_e = \left(\frac{6}{\omega}\right)\frac{(V_{TH})^2}{\left(R_{TH}+\frac{r}{2s-1}\right)^2+(X_{TH}+2x_q)^2}\left(\frac{r}{2s-1}\right) \text{ N-m} \quad (67)$$

XI. TORQUE/SLIP CHARACTERISTICS OF 3-PHASE TRANSFER FIELD MOTOR

The torque/slip characteristic of the motor is analysed using equation 67 for the Matlab plot, as shown in figure 12.

XII. EFFICIENCY/SLIP CHARACTERISTICS OF 3-PHASE TRANSFER FIELD MOTOR

The efficiency/slip relationship for 3-phase transferred field machine can be investigated using the per phase steady-state equivalent circuit of a 3-phase transfer field motor of fig 10(b).

From fig 10(b);

The input impedance looking through the input terminals is;

$$Z = r + j2x_q + \left[\frac{j(X_{md}-X_{mq})\left(j2x_q+\frac{r}{2s-1}\right)}{\frac{r}{2s-1}+j\left(2x_q+(X_{md}-X_{mq})\right)}\right] \quad (68)$$

Also, the current in the main winding (I_A) is given by;

$$I_A = \frac{V_A}{Z} \quad (69)$$

The current in the auxiliary winding is given by;

$$I_a = \left[\frac{j(X_{md}-X_{mq})}{\frac{r}{2s-1}+j\left(2x_q+(X_{md}-X_{mq})\right)}\right] I_A \quad (70)$$

The copper losses in the main and auxiliary windings $= 3r(I_A + I_a)^2$ (71)

Input power = Output power + the copper losses, excluding windage and friction losses.

From equation 57,

The machine input power $= 6r\left(\frac{1-s}{2s-1}\right)(I_a)^2 + 3r(I_A + I_a)^2$

$$= 3r\left[2\left(\frac{1-s}{2s-1}\right)(I_a)^2 + (I_A+I_a)^2\right] \quad (72)$$

Hence, the machine Efficiency $\varepsilon = \frac{output\ power}{input\ power} =$

$$\frac{2\left(\frac{1-s}{2s-1}\right)(I_a)^2}{2\left(\frac{1-s}{2s-1}\right)(I_a)^2+(I_A+I_a)^2} \quad (73)$$

The efficiency/slip characteristics of 3-phase transfer field motor is analysed using equation 73 for the Matlab plot as shown in figure 13

Table 1: The Machine Parameters

S/No	Parameter	Value
1	L_{md}	133.3mH
2	L_{mq}	25.6mH
3	$L_{Ls} = L_{ia} = L_{er}$	0.6mH
4	$r_m = r_a$	3.0Ω
5	J	$1.98\text{x}10^{-3}\text{kgm}^3$
6	V	220V
7	F	$50H_Z$
8	P	2

The Matlab plots for the torque developed against slips are shown in figure 4.1a and 4.1b

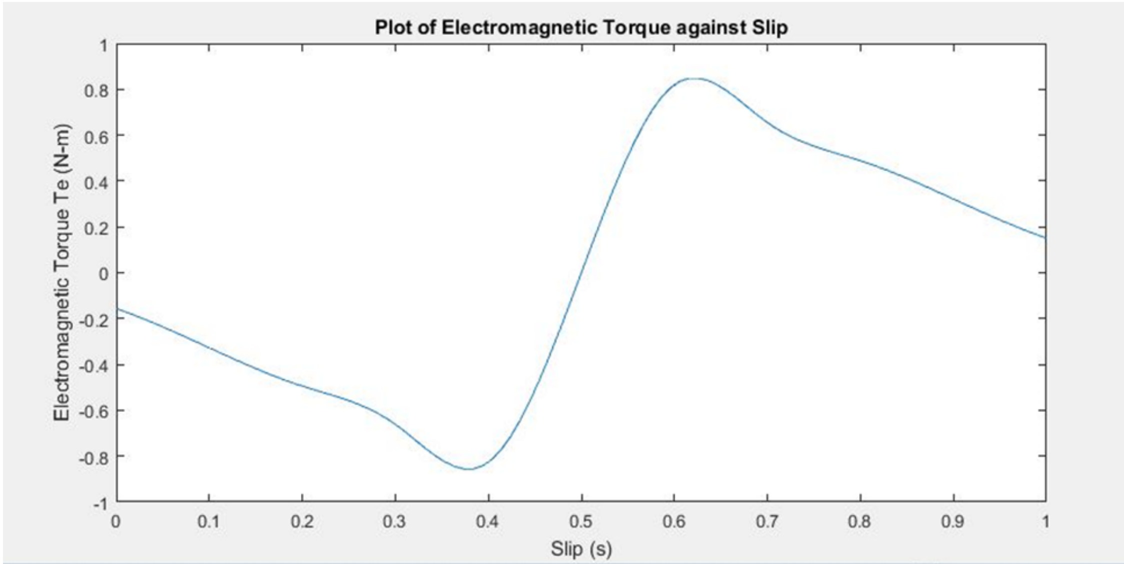

Fig 12 A plot of torque developed against ranges of slip(s) for 3-phase transfer field motor

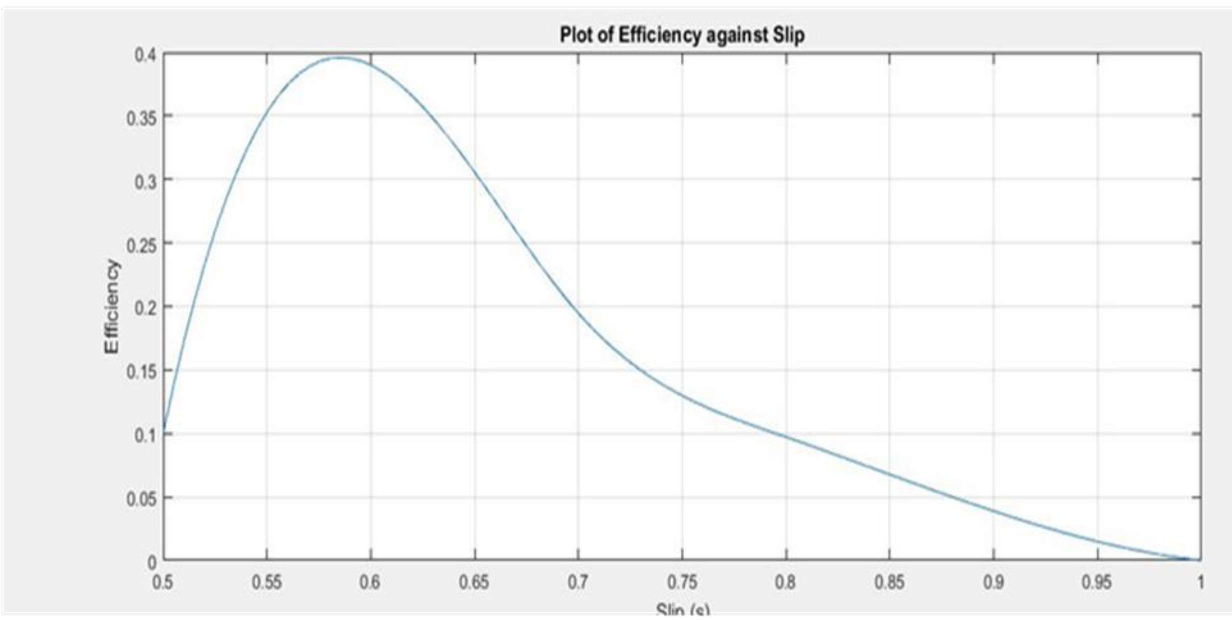

Fig 13: Efficiency/Slip characteristics of 3-phase transferred field motor

XIII. Power factor/slip characteristics of 3-phase transferred field reluctance motor

The Matlab plots of the power factor (cos θ)/slip relationships for 3-phase transferred field motors is obtained using equations 75. The plot is depicted in figure 14.

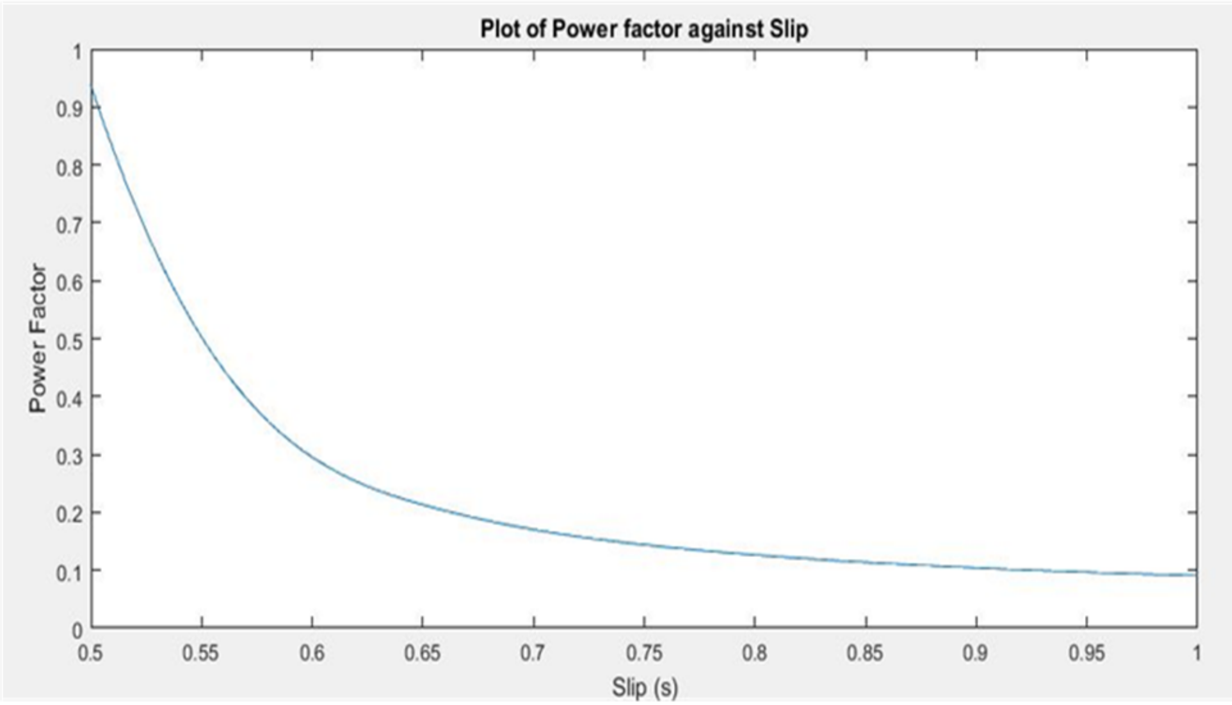

Fig. 14: Power factor/slip characteristics of 3-phase transfer field motor.

XIV. Induced current/slip characteristics of 3-phase transfer field motor

The Matlab plots of the induced current (I_a and I_{23})/slip relationship for the motor is obtained using equations 64. The matlab plot is shown in figure 15.

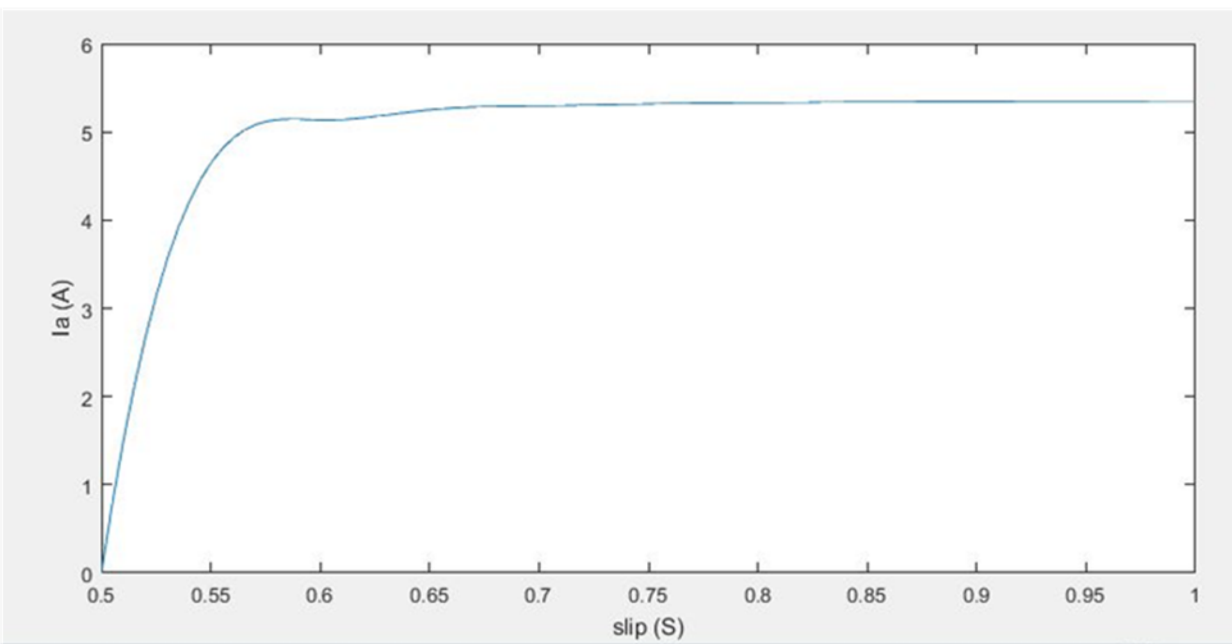

Figure 15: A plot of auxiliary current against slip for 3-phase transfer field motor with no cage winding.

XV. Dynamic-state simulations of 3-phase transfer field motor

Using equation 26 through equation 46 and values for circuit parameters of table 1, the dynamic simulation plots of 3-phase transfer field motor are shown in figure 16 and figure 17.

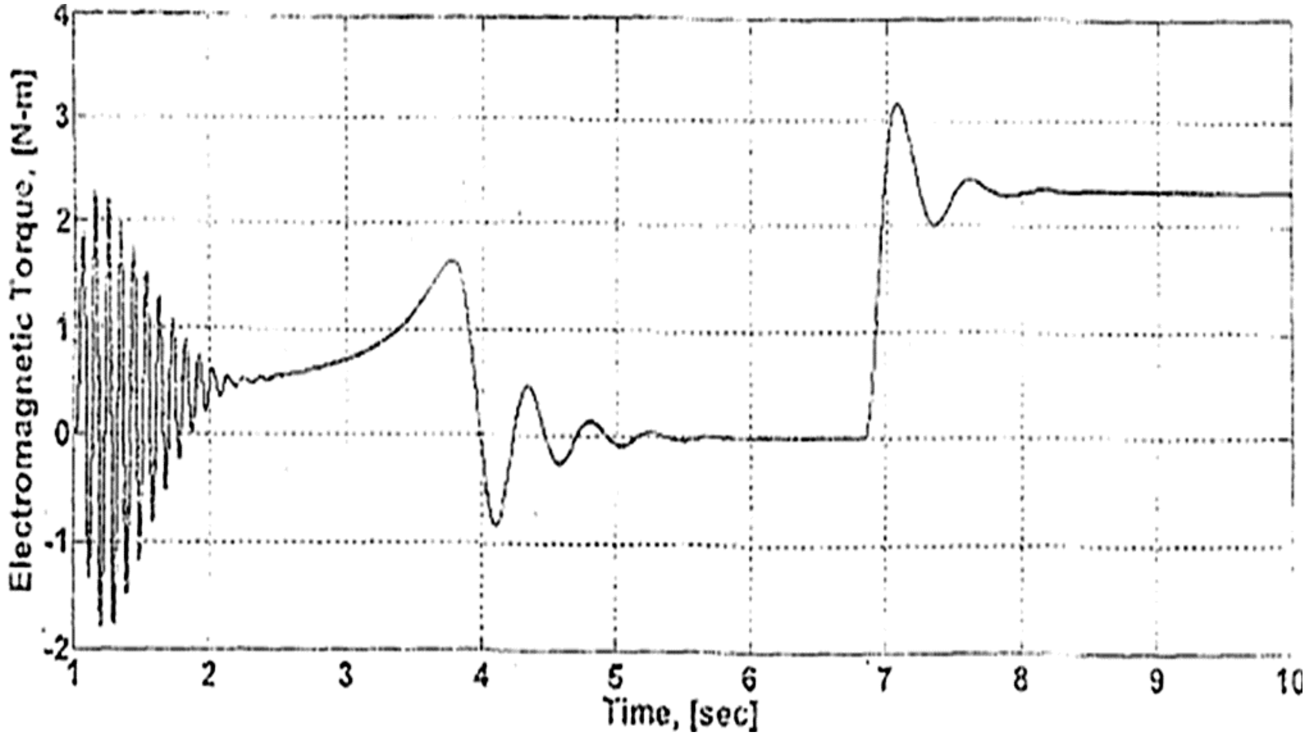

Fig. 16: The Electromagnetic Torque against time of three-phase transfer field motor.

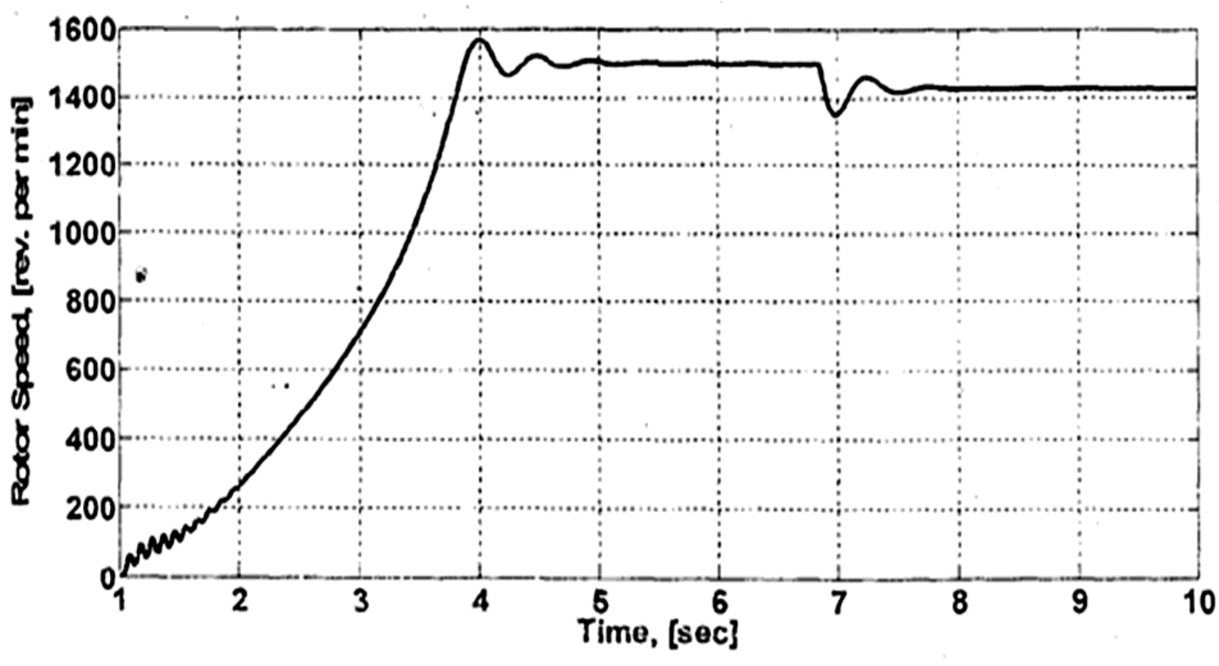

Fig 17: Auxiliary winding (rotor) speed (ω_r) against time of three-phase transfer field motor.

ANALYSIS OF RESULTS

i. For Steady-state operation, from the steady-state electromagnetic torque versus slip characteristics of figure 12 at slip of 0.5, the injected voltage at the auxiliary and winding is zero. Hence, necessitating a zero torque. The starting torques of the steady-state electromagnetic torque of the machine is 0.16N-m while the maximum 0.80N-m.

   At stand still condition of the machine, the power factor is seen to be 0.09 as in fig.14. These are indeed poor, compared to output characteristics of induction motor of comparable size and rating. Also, at synchronous speed (s = 0.5), current decayed to zero, but at zero speed (Nr = 0, S = 1), starting current is a maximum at 5.3A as in figure (15).

ii. For the dynamic operation of the motor, the rotor speed run-up plot against time is shown in figure 17. There was a little transient at different stages while rotor speed builds up before an application of load at 7 seconds. After another little transient, the rotor speed now settles at a steady-state at about 1415N-m. Also, the plot of Electromagnetic torque against time for the motor, with oscillation noticed at different stages is shown in figure 16. A close observation shows that on no-load, value for electromagnetic torque is zero. One application of load torque at 6.8second to the motor, it oscillates and settled at a steady-state of 2.25N-m

REFERENCES

[1] Agu, L. A. (1984). Output enhancement in the transfer-field machine using rotor circuit induced currents. *Nigeria Journal of Technology* Vol. 8, No. 1. Pp. 7 – 11.

[2] Anih, L. U. and Agu, L.A. (2008). Mechanism of Torque Production in a coupled polyphase reluctance machine. Nigerian Journal of Technology vol. 27 No.1. Pp 29-38.

[3] Anih L.U, Obe, E.S (2009). Performance analysis of a composite dual winding reluctance machine. Energy conversion and management 50(2009) 3056-3062

[4] Chee-mun O. (1997). *Dynamic Simulation of Electric Machinery using Matlab/simulink*. Prentice Hall PTR, New Jersey.

[5] Eleanya, M.N. (2015). *Comparative Analysis of a transfer field machine and induction machine*. Thesis submitted to the Department of Electrical Engineering University of Nigeria Nsukka pp 72

[6] Ijeomah, C. N. et al (1996). “Torque enhancement of a reluctant effect machine by step-frequency secondary voltage injection method”. Unpublished Master of Engineering Thesis, University of Nigeria, Nsukka.